



Rigby, M., Montzka, S. A., Prinn, R. G., White, J. W. C., Young, D., O'Doherty, S., Lunt, M. F., Ganesan, A. L., Manning, A. J., Simmonds, P. G., Salameh, P. K., Harth, C. M., Mühle, J., Weiss, R. F., Fraser, P. J., Steele, L. P., Krummel, P. B., McCulloch, A., & Park, S. (2017). Role of atmospheric oxidation in recent methane growth. *Proceedings of the National Academy of Sciences of the United States of America*, 114(21), 5373-5377. <https://doi.org/10.1073/pnas.1616426114>

Peer reviewed version

Link to published version (if available):
[10.1073/pnas.1616426114](https://doi.org/10.1073/pnas.1616426114)

[Link to publication record in Explore Bristol Research](#)
PDF-document

This is the author accepted manuscript (AAM). The final published version (version of record) is available online via PNAS at <http://www.pnas.org/content/early/2017/04/11/1616426114>. Please refer to any applicable terms of use of the publisher.

University of Bristol - Explore Bristol Research

General rights

This document is made available in accordance with publisher policies. Please cite only the published version using the reference above. Full terms of use are available: <http://www.bristol.ac.uk/red/research-policy/pure/user-guides/ebr-terms/>

The role of atmospheric oxidation in recent methane growth

Matt Rigby^{a,1}, Stephen A. Montzka^b, Ronald G. Prinn^c, James W. C. White^d, Dickon Young^a, Simon O'Doherty^a, Mark Lunt^a, Anita L. Ganesan^e, Alistair Manning^f, Peter Simmonds^a, Peter K. Salameh^g, Chris M. Harth^g, Jens Mühle^g, Ray F. Weiss^g, Paul J. Fraser^h, L. Paul Steele^h, Paul B. Krummel^h, Archie McCulloch^a, and Sunyoung Parkⁱ

^aSchool of Chemistry, University of Bristol, Bristol, BS8 1TS, UK; ^bNational Oceanic and Atmospheric Administration, Earth System Research Laboratory, Boulder, Colorado, 80303, USA; ^cCenter for Global Change Science, Massachusetts Institute of Technology, Cambridge, Massachusetts, 02139, USA; ^dInstitute of Arctic and Alpine Research, University of Colorado, Boulder, Colorado, 80309, USA; ^eSchool of Geographical Sciences, University of Bristol, Bristol, BS8 1SS, UK; ^fHadley Centre, Met Office, Exeter, EX1 3PB, UK; ^gScripps Institution of Oceanography, University of California, San Diego, La Jolla, CA 92093, USA; ^hCSIRO Oceans and Atmosphere, Climate Science Centre, Aspendale, Victoria 3195, Australia; ⁱDepartment of Oceanography, Kyungpook National University, Sangju 742-711, Republic of Korea

This manuscript was compiled on February 28, 2017

The growth in global methane (CH₄) concentration, which had been ongoing since the industrial revolution, stalled around the year 2000, before resuming globally in 2007. We evaluate the role of the hydroxyl radical (OH), the major CH₄ sink, in the recent CH₄ growth. We also examine the influence of systematic uncertainties in OH concentrations on CH₄ emissions inferred from atmospheric observations. We use observations of 1,1,1-trichloroethane (CH₃CCl₃), which is lost primarily through reaction with OH, to estimate OH levels as well as CH₃CCl₃ emissions, whose uncertainty has previously limited the accuracy of OH estimates. We find a 64% - 70% probability that a decline in OH has contributed to the post-2007 methane rise. Our median solution suggests that CH₄ emissions increased relatively steadily during the late 1990s and early 2000s, after which, growth was more modest. This solution obviates the need for a sudden, statistically significant change in total CH₄ emissions around the year 2007 to explain the atmospheric observations, and can explain some of the decline in the atmospheric ¹³CH₄/¹²CH₄ ratio and the recent growth in C₂H₆. Our approach indicates that significant OH-related uncertainties in the CH₄ budget remain, and we find that it is not possible to implicate, with a high degree of confidence, rapid global CH₄ emissions changes as the primary driver of recent trends, when our inferred OH trends and these uncertainties are considered.

Methane | Hydroxyl radical | Methyl chloroform | Isotope

Methane (CH₄), the second most important partially anthropogenic greenhouse gas, is observed to vary markedly in its year-to-year growth rate (Figure 1). The causes of these variations have been the subject of much controversy and uncertainty, primarily because there are a wide range of poorly quantified sources and because its sinks are ill-constrained[1]. Of particular recent interest is the cause of the “pause” in CH₄ growth between 1999 and 2007, and the renewed growth from 2007 onwards[2–7]. It is important that we understand these changes if we are to better project future CH₄ changes and effectively mitigate enhanced radiative forcing due to anthropogenic methane emissions.

The major sources of CH₄ include wetlands (natural and agricultural), fossil fuel extraction and distribution, enteric fermentation in ruminant animals and solid and liquid waste. Our understanding of the sources of CH₄ come from two approaches: “bottom-up”, in which inventories or process models are used to predict fluxes, or “top-down”, in which fluxes are inferred from observations assimilated into atmospheric chemical transport models. Bottom-up methods suffer from uncertainties and potential biases in the available activity data or emissions factors, or the extrapolation to large scales of a

relatively small number of observations. Furthermore, there is no constraint on the global total emissions from bottom-up techniques. The top-down approach is limited by incomplete or imperfect observations and our understanding of atmospheric transport and chemical sinks. For CH₄, these difficulties result in a significant mismatch between the two methods [1].

The primary CH₄ sink is the hydroxyl radical (OH) in the troposphere, although smaller sinks also exist, such as methanotrophic bacteria in soils, oxidation by chlorine radicals in the marine boundary layer and photochemical destruction in the stratosphere. Predictions of the magnitude and variability of OH in the current generation of atmospheric models have been shown to be diverse[8]. Furthermore, due to its short lifetime, it is difficult to infer global OH concentrations using direct observations. Therefore, indirect observational methods are needed. The most commonly used approach has been to monitor the trends in 1,1,1-trichloroethane (CH₃CCl₃), whose major sink is reaction with OH, and, by making assumptions about its emissions into the atmosphere, infer global OH concentrations[9–13]. Recent work using this approach indicated that OH changes could have played a role in the pause in CH₄ that occurred after 1998 [3, 14].

Previous studies have shown that OH trends inferred using

Significance Statement

Methane, the second most important greenhouse gas, has varied markedly in its atmospheric growth rate. The cause of these fluctuations remains poorly understood. Recent efforts to determine the drivers of the pause in growth in 1999 and renewed growth from 2007 onwards have focused primarily on changes in sources alone. Here we show that changes in the major methane sink, the hydroxyl radical, have likely played a substantial role in the global methane growth rate. This work has significant implications for our understanding of the methane budget, which is important if we are to better predict future changes in this potent greenhouse gas, and effectively mitigate enhanced radiative forcing due to anthropogenic emissions.

MR devised and carried out the research and wrote the manuscript. SAM and RGP helped to devise the research, provided data and contributed to the writing of the manuscript. JWCW, DY, SOD, PS, PKS, CMH, JM, RFW, LPS, PJF, PBK and SP contributed observations and helped with the writing of the manuscript. MFL, AG and AM carried out a regional analysis of the CH₃CCl₃ observations. AMC provided guidance on the CH₃CCl₃ emissions model.

The authors declare no conflicts of interest.

¹To whom correspondence should be addressed. E-mail: matt.rigby@bristol.ac.uk

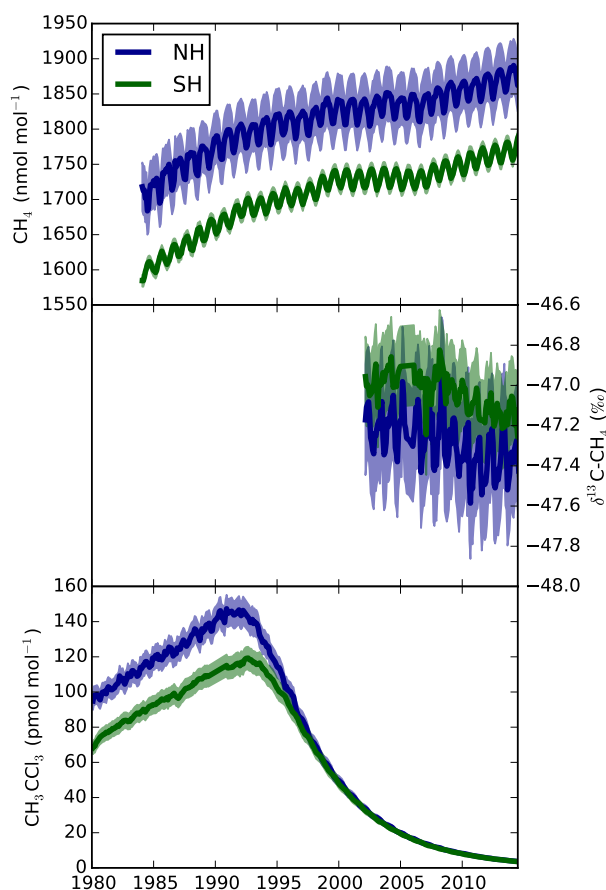


Fig. 1. First panel: NOAA observations of CH_4 ; second panel: INSTAAR observations of $\delta^{13}\text{C}-\text{CH}_4$; third panel: AGAGE observations of CH_3CCl_3 . Each plot shows the northern hemisphere (NH) and southern hemisphere (SH) mean, and shading indicates the assumed 1-sigma model and measurement uncertainty, as defined in the SI Materials and Methods.

CH_3CCl_3 could be highly sensitive to systematic errors in the assumed emissions trends, particularly in the 1980s and early 1990s when emissions were changing rapidly [15]. Some authors have attempted to reduce this source of uncertainty by including CH_3CCl_3 emissions as part of the inversion [12]. However, these studies assumed that emissions uncertainties were Gaussian and uncorrelated between years, potentially reducing the impact of systematic errors in the *a priori* emissions model. Furthermore, with a few exceptions [16], most work has derived OH separately to CH_4 and its global $^{13}\text{C}/^{12}\text{C}$ source signature, limiting the propagation of uncertainty in OH through to the derived CH_4 fluxes. The inability to quantify CH_3CCl_3 systematic emissions uncertainties may be particularly problematic in recent years, when, as a result of its production and consumption ban under the Montreal Protocol, reported consumption has dropped to very low levels, but evidence of continued emissions can still be seen in atmospheric observations (Figure S1) [17, 18]. Therefore, the assumptions that were used in early estimates of CH_3CCl_3 emissions, which were based on industry surveys at a time when CH_3CCl_3 was widely used [19], are unlikely to hold in recent decades.

In contrast to previous approaches, the method used in this

paper explicitly includes a model of the CH_3CCl_3 emissions processes in the estimation scheme. Information regarding the global emissions of long-lived trace gases such as CH_3CCl_3 can be derived simultaneously with their atmospheric sinks, by jointly considering factors such as the long-term trend in concentration and the inter-hemispheric gradient [20]. We extend this approach here by including the uncertain emissions and atmospheric model parameters jointly in a hierarchical Bayesian estimation framework that is informed by atmospheric data from multiple species. This ensures that uncertainties in each component are propagated throughout the system. A full list of model parameters explored in the inversion is given in Table S1.

In order to focus on the uncertainties in the CH_3CCl_3 emissions model, we chose to use a computationally efficient “box model” of atmospheric transport and chemistry that included two tropospheric boxes and one stratospheric box. Previous authors have noted that the use of atmospheric box models with annually repeating transport can cause erroneous fluctuations in derived OH concentrations over periods of around three years or less, particularly during periods when emissions of CH_3CCl_3 were relatively large [15]. However, recent studies have shown that, at least in recent years when atmospheric CH_3CCl_3 gradients are small, OH inversions based on box models agree very closely (to within $\sim 1\%$) with three-dimensional model inversions using analysed meteorology [13], or that OH variations derived using box models can be used to simulate realistic CH_3CCl_3 trends using three-dimensional models [14]. Therefore, in this paper, we primarily focus on longer-term OH trends, and we expect that our findings for recent decades would not be substantially different if a more complex model were used.

The atmospheric and emissions model parameters were constrained in a multi-species inversion using monthly mean observations of atmospheric CH_3CCl_3 from both the Advanced Global Atmospheric Gases Experiment (AGAGE) [21] and National Oceanic and Atmospheric Administration (NOAA) [4, 13] networks, along with NOAA CH_4 data and $^{13}\text{C}-\text{CH}_4$ observations from the University of Colorado’s Institute of Arctic and Alpine Research (INSTAAR) [22, 23] (Figures 1). Co-located AGAGE and NOAA observations were found exhibit somewhat different long-term CH_3CCl_3 trends. Therefore, two sets of inversions were performed, based on the CH_3CCl_3 observations from each network (Figure S2). AGAGE CH_4 observations were not used in the main part of this study as they were found to agree very closely with NOAA data, but cover a shorter time period. Further details of about the observations are provided in the supplementary materials and methods, and the the site locations are shown in Table S2.

Results

The first two panels of Figure 2 show the simultaneously-derived OH concentrations and CH_3CCl_3 emissions inferred from independent application of our approach using AGAGE or NOAA observations. A comparison between the observations and the model is shown Figure S3 and numerical values for quantities in the figure are provided in the Supplement. The median solution shows a relatively small OH trend in the 1980s and 1990s (with smaller inter-annual variability than previous CH_3CCl_3 inversions [11, 12, 24]), followed by an upward trend in OH concentration on the order of 10% from the late 1990s

249 to 2004 ($11 \pm 13\%$ and $9 \pm 12\%$ increase for AGAGE and
250 NOAA, respectively, between 1998 and 2004). This trend is
251 of a similar size to those highlighted in previous studies using
252 CH_3CCl_3 [14, 24]. Post-2004, our median estimate shows a
253 decline in OH. This finding would suggest that at least some
254 fraction of the post-2007 CH_4 growth could be attributable to
255 declining OH. By carrying out a set of linear regressions on
256 the post-2007 OH estimates from our *a posteriori* ensemble
257 of model states, we find a 70% or 64% probability that OH
258 exhibited some level of negative trend during this period, when
259 AGAGE or NOAA data were used, respectively (the mean
260 difference between the 2004 and 2014 OH concentrations was -8
261 $\pm 11\%$ and $-11 \pm 11\%$, respectively). In addition to this trend
262 are several features of our OH inversion that are important
263 to note. Firstly, significant uncertainties remain in the global
264 OH concentration, such that it is possible to draw a “constant
265 OH” line that is consistent with the observation-derived OH,
266 within its uncertainties. Secondly, small differences in the
267 CH_3CCl_3 trend and inter-hemispheric gradient measured by
268 the two independent networks lead to variations in the derived
269 OH concentration and CH_3CCl_3 emissions. However, these
270 differences are small compared to the other uncertainties in
271 the system.

272 Differences between our derived CH_3CCl_3 emissions and
273 those assumed previously (Figure 2, second panel) explain part
274 of the discrepancy between our OH trends and those derived in
275 previous studies (Figure 2, first panel), although other factors
276 such as the treatment of the ocean sink also contribute (see SI
277 text). Our global CH_3CCl_3 emissions estimates differ to the
278 previous estimates shown in the Figure in that they have been
279 adjusted in the inversion to be consistent with atmospheric ob-
280 servations (and in particular, the inter-hemispheric CH_3CCl_3
281 mole fraction gradient), instead of being imposed based on
282 bottom-up models or an assumed rate of decline [13, 24]. The
283 CH_3CCl_3 emissions derived in our inversion indicate that there
284 was ongoing release of CH_3CCl_3 to the atmosphere, at least
285 through 2014, despite national reports indicating that use of
286 this substance ceased in 2013[25]. Analysis of high-frequency
287 AGAGE data confirms that emissions persisted throughout
288 this period, upwind of some monitoring sites (Figure S1).

289 In addition to our multi-species inversion, we carried out an
290 inversion for OH concentrations and CH_3CCl_3 emissions using
291 only CH_3CCl_3 observations (Figure S4). We find that the OH
292 concentrations and variability derived in this analysis leads to
293 a similar result to the multi-species inversion, indicating that
294 the constraint on OH is primarily from CH_3CCl_3 , rather than
295 CH_4 and its $^{13}\text{C}/^{12}\text{C}$ ratio. Therefore, the timing of the rise
296 and fall in inferred OH has not been significantly influenced
297 by “knowledge” of the pause and renewed growth in CH_4 .

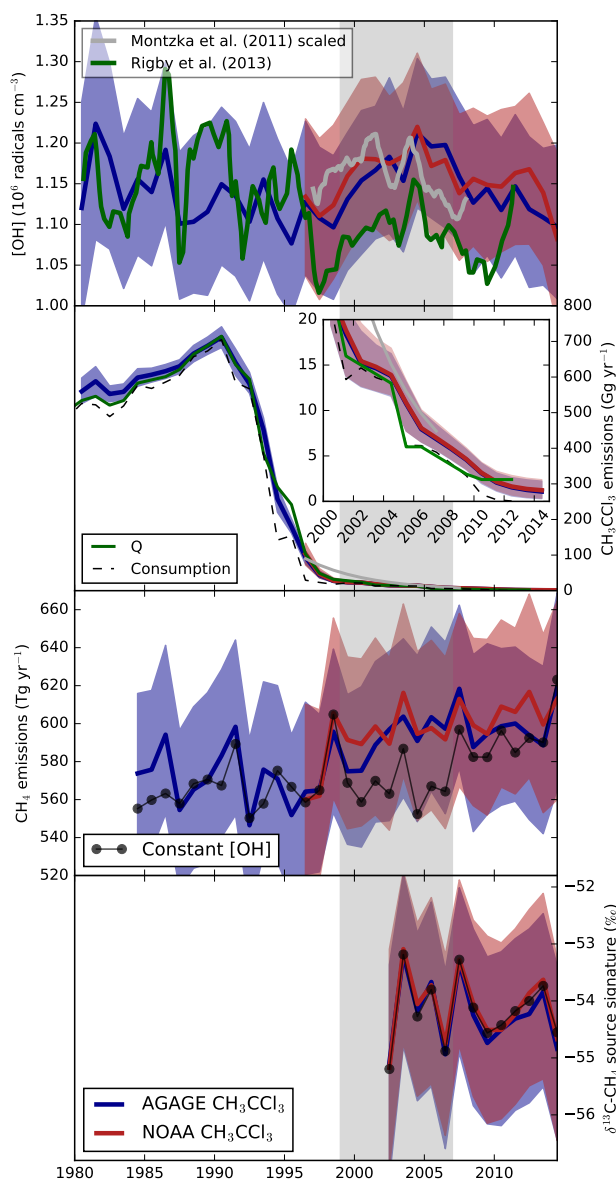
299 Our multi-species inversion allows us to propagate infor-
300 mation on the derived OH concentration, and its uncertainty,
301 through to estimates of CH_4 emissions. We find that, similarly
302 to OH concentration, it is possible to draw a “constant CH_4
303 emissions” line within the derived uncertainties (Figure 2, third
304 panel). However, the median solution suggests a relatively
305 steady upward trend from the mid-1990s to the mid-2000s,
306 followed by a period of smaller growth. We note that our result
307 does not require a sudden, statistically significant, increase in
308 CH_4 emissions in 2007, as suggested elsewhere, to explain the
309 observations[5–7, 26, 27]. Instead, it is implied that the rise
310 in atmospheric mole fractions in 2007 is consistent with the

decline in OH concentrations post-2004, overlaid on a grad- 311
ual rise in CH_4 emissions with some additional inter-annual 312
variability on the order of 10 Tg yr^{-1} . 313
314
315
316
317
318
319
320
321
322
323
324
325
326
327
328
329
330

The third panel in Figure 2 also shows an inversion where
OH is constrained to be inter-annually repeating. In this sce- 331
nario, CH_4 emissions remain at a relatively low level through- 332
out the 2000s, compared to the varying-OH inversions, until 333
around 2007, when they sharply increase. Compared to the 334
5-year period before 2007, emissions from 2007 to 2011 (inclu- 335
sive) were $22 \pm 9 \text{ Tg yr}^{-1}$ higher in this scenario (similarly to 336
other studies that had assumed constant OH[28]). In contrast, 337
for the inversions with the OH changes derived from AGAGE 338
or NOAA CH_3CCl_3 , this difference was found to be $4 \pm 23 \text{ Tg}$ 339
 yr^{-1} or $9 \pm 22 \text{ Tg yr}^{-1}$, respectively. 340
341
342
343
344
345
346
347
348
349
350
351
352
353
354
355
356
357

In our inversion, we determine the global $^{13}\text{CH}_4/^{12}\text{CH}_4$ 358
source signature that would be required to match the observed 359
atmospheric $\delta^{13}\text{C}-\text{CH}_4$ (see SI materials and methods), con- 360
sidering changes in OH and global CH_4 emissions (Figure 361
2, fourth panel). The observations and modeling framework 362
provide relatively weak constraints on this term, such that 363
the uncertainties on annual $^{13}\text{CH}_4/^{12}\text{CH}_4$ source ratios are 364
around an order of magnitude larger, at around 1%, than the 365
changes that would be required to match the observed trends, 366
which are of the order of 0.1%. Furthermore, we find that, due 367
to the very long timescales over which methane isotopologues 368
respond to source or sink perturbations[29], our derived source 369
ratio values are significantly auto-correlated, meaning that, in 370
our inversion, the derived annual values cannot be considered 371
fully independent of one another (Figure S5). 372

373
374
375
376
377
378
379
380
381
382
383
384
385
386
387
388
389
390
391
392
393
394
395
396
397
398
399
400
401
402
403
404
405
406
407
408
409
410
411
412
413
414



415 **Fig. 2.** First panel: inferred tropospheric annual mean OH concentration; second
416 panel: global CH_3CCl_3 emissions; third panel: global CH_4 emissions; fourth panel:
417 global $^{13}\text{C}/^{12}\text{C}$ source isotope ratio of CH_4 . The blue lines and shading show
418 quantities inferred when AGAGE CH_3CCl_3 were used, and red lines and shading
419 shows those inferred using NOAA CH_3CCl_3 . Lines indicate the median and the
420 shading shows the 16th to 84th percentile (approximately ± 1 sigma). The green and
421 grey lines in the top two panels show estimates from previous studies that used the
422 same observations, but different methodologies and emissions[13, 24]. The black line
423 in the lower two panels shows the methane and isotopologue changes inferred when
424 inter-annually repeating OH was used. The grey shading shows the approximate
425 start and end of the methane “pause”. Numerical values for the top two panels are
426 available in the Supplementary Material.

427 Discussion

428 We have presented an inversion that derives global OH concentrations
429 simultaneously with CH_3CCl_3 and CH_4 emissions and the $^{13}\text{C}/^{12}\text{C}$
430 source isotope ratio of CH_4 . The blue lines and shading show
431 quantities inferred when AGAGE CH_3CCl_3 were used, and red lines and shading
432 shows those inferred using NOAA CH_3CCl_3 . Lines indicate the median and the
433 shading shows the 16th to 84th percentile (approximately ± 1 sigma). The green and
434 grey lines in the top two panels show estimates from previous studies that used the
435 same observations, but different methodologies and emissions[13, 24]. The black line
436 in the lower two panels shows the methane and isotopologue changes inferred when
437 inter-annually repeating OH was used. The grey shading shows the approximate
438 start and end of the methane “pause”. Numerical values for the top two panels are
439 available in the Supplementary Material.

435 have contributed to the recent pause and growth in CH_4 , as
436 reflected in the median CH_4 emissions, which only change slowly
437 after the late 1990s. In contrast, our “constant OH” inversion
438 shows a relatively sudden emissions increase in 2007. It is inter-
439 esting to note that these two sets of derived emissions agree
440 relatively well during the 1990s (at levels of approximately
441 560 Tg yr^{-1}), and after 2010 (approximately 600 Tg yr^{-1}),
442 but the trajectory of the transition is different, with most
443 of the increase occurring in the late 1990s if OH is allowed
444 to change, but primarily around 2007 if it isn’t. However,
445 it is also important to note that the median solution of the
446 constant OH inversion falls within the 1-sigma range of the
447 “varying OH” inversions.

448 Notwithstanding the uncertainties, our findings are in con-
449 trast to recent work in which a three-dimensional model of
450 atmospheric transport and chemistry predicted only a gradual
451 decrease in methane lifetime over the last three decades, and
452 therefore that emissions changes were primarily responsible for
453 the CH_4 growth[7]. We also provide an alternative perspective
454 to another study that attributed much of the recent growth
455 in CH_4 and $\delta^{13}\text{C}-\text{CH}_4$ to tropical wetland emissions, based
456 partly on the finding that there was no clear signal of an
457 OH change in other reduced chemical tracers (CH_3CCl_3 had
458 not been considered)[6]. Other authors had investigated and
459 ruled-out OH changes as being the sole driver of recent trends,
460 in studies that used $\delta^{13}\text{C}-\text{CH}_4$ and ethane (C_2H_6) to assign
461 the growth in methane to livestock and oil and gas extraction,
462 respectively[5, 26].

463 Forward model simulations with our derived OH and a con-
464 stant $^{13}\text{C}-\text{CH}_4$ source show a decline in atmospheric $\delta^{13}\text{C}-\text{CH}_4$
465 post-2006, demonstrating that OH trends likely contributed
466 to the recent $\delta^{13}\text{C}-\text{CH}_4$ trends in our inversion (Figure S6).
467 Whilst the precise contribution of OH to the observed trend
468 is difficult to isolate from other influences, it is likely that our
469 derived changes are not sufficient to explain the entire recent
470 decline in $\delta^{13}\text{C}-\text{CH}_4$, and that some change in the source sig-
471 nature has also occurred, as has been suggested previously[26].
472 However, as described above, the uncertainties on the source
473 signature in our inversion are much larger than the required
474 change in source signature, making the precise identification
475 of a change in one or more source sectors difficult.

476 Some recent studies have pointed to an “upturn” in global
477 concentrations of ethane (C_2H_6), coincident with the recent
478 rise in CH_4 [5, 30, 31], which may imply an increase in CH_4
479 emissions due to an increase in oil and gas extraction. Column
480 averaged measurements in the background atmosphere reveal
481 trends in C_2H_6 between 2007 and 2014 of $23 (18, 28) \text{ pmol}$
482 $\text{mol}^{-1} \text{ yr}^{-1}$ and $-4 (-6, -1) \text{ pmol mol}^{-1} \text{ yr}^{-1}$ (95 percent
483 confidence intervals) in the northern and southern hemispheres,
484 respectively[5]. Because C_2H_6 is primarily removed from the
485 atmosphere via reaction with OH, we also expect changes
486 in OH to have an impact on C_2H_6 concentrations, even if
487 emissions have not changed. By running our model forward
488 with constant C_2H_6 emissions (which were tuned to match
489 the mean northern and southern hemispheric observed mole
490 fractions[5], Figure S7) and our derived OH concentrations,
491 we find that it is possible to explain a global background
492 C_2H_6 growth rate of $9 (-11, 30) \text{ pmol mol}^{-1} \text{ yr}^{-1}$ and $3 (-4,$
493 $11) \text{ pmol mol}^{-1} \text{ yr}^{-1}$ (95 percent confidence interval) in the
494 northern and southern hemispheres respectively from 2007 to
495 2014. The timing of transition from declining to growing C_2H_6
496

497 mole fractions in the northern hemisphere coincides to within
498 one or two years with change from growing to declining OH in
499 our inversion (Figure S7). Therefore, it is possible that some
500 of the recent upturn in northern hemispheric C₂H₆ is also
501 due to changes in OH concentration. Our constant emissions
502 simulation does not match the continued downward trend in
503 southern hemispheric C₂H₆, although the uncertainties in our
504 estimates overlap with the observed trend.

505 As we stress above, it is important to note the magnitude of
506 the uncertainties in our inversions, which we believe are more
507 comprehensive than previous work, as they incorporate several
508 systematic factors, particularly relating to CH₃CCl₃ emissions.
509 If OH changes and their uncertainty are not considered, a
510 sudden and statistically significant increase in CH₄ emissions
511 after 2006 is required to fit the observations. Whilst we cannot
512 rule out this scenario, in our inversions in which the recent
513 CH₃CCl₃ budget is objectively considered, a trajectory in
514 which CH₄ emissions have changed more gradually during the
515 late 2000s is also plausible. Our study highlights that, without
516 careful consideration of the CH₄ sink and its uncertainty, it
517 would be possible to draw misleading conclusions regarding
518 the emissions trend when long-term records of background
519 atmospheric observations are used. Our median estimate
520 suggests an important role for OH in the recent CH₄ pause
521 and growth, overlaid on a relatively gradual increase in CH₄
522 emissions over the last two decades.

524 Materials and Methods

525 Atmospheric mole fractions were simulated using a box model atmo-
526 sphere, which accounted for mixing between the two tropospheric
527 hemispheres, and exchange with the stratosphere. Loss of CH₃CCl₃
528 and CH₄ occurred primarily through reaction with OH in the model
529 troposphere (with the potential for differences in the northern and
530 southern OH concentration[32]). The model also included a first-
531 order loss of each compound in the stratosphere (all stratospheric
532 losses were considered to contribute to a single stratospheric loss
533 rate), first-order sinks for CH₄ in the troposphere due to reac-
534 tion with chlorine and uptake by methanotrophs in soils[1], and
535 an ocean uptake for CH₃CCl₃ according to previous ocean model
536 estimates[33]. Isotopic fractionation of CH₄ was assumed to oc-
537 cur for each sink based on recent estimates [34–37]. Emissions
538 of CH₃CCl₃ were estimated using a model that took as an input
539 consumption or use of CH₃CCl₃. Uncertain parameters in the
540 atmospheric and emissions model were estimated in the inversion,
541 along with estimates of the annual, hemispheric CH₄ surface flux
542 and ¹³CH₄/¹²CH₄ source signature and global, annual OH concen-
543 tration. By exploring some of the major unknown parameters in
544 this multi-species framework, the influence of uncertainties in each
545 parameter and the atmospheric data could be propagated through
546 the system (see Table S1 for a list of model parameters). AGAGE,
547 NOAA and INSTAAR data (Figure 1) were used to constrain
548 the model parameters using a hierarchical Bayesian framework,
549 which was solved using a Markov Chain Monte Carlo (MCMC)
550 algorithm[38]. The MCMC approach iteratively explores model
551 states, randomly accepting or rejecting proposed parameter values
552 with a probability dependent on the ratio of posterior probability
553 density of the “current” and proposed states. The outcome is a chain
554 of parameter values that span the posterior probability density func-
555 tions. Atmospheric data from a subset of the three networks were
556 used, where predominantly “background” (unpolluted) air masses
557 were sampled, and where time series of the order of a decade or
558 more were available (SI Text). The delta notation for observations
559 of ¹³C/¹²C ratio in CH₄ is defined as:

$$\delta^{13}\text{C} - \text{CH}_4 = 1000 \left(\frac{R}{R_{std}} - 1 \right) \quad [1]$$

557 where R is the ¹³C/¹²C ratio in CH₄, and R_{std} refers to a reference
558 ratio[39] and values are quoted in per mille (‰). Further details

are provided in the SI Text.

ACKNOWLEDGMENTS. Matt Rigby is supported by a NERC
Advanced Research Fellowship (NE/I021365/1). The operations
of the AGAGE instruments at Mace Head, Trinidad Head, Cape
Matatula, Ragged Point, and Cape Grim are supported by the
National Aeronautics and Space Administration (NASA) (grants
NAG5-12669, NNX07AE89G, and NNX11AF17G to MIT and grants
NNX07AE87G, NNX07AF09G, NNX11AF15G, and NNX11AF16G
to SIO), the Department of Energy and Climate Change (DECC,
UK) contract GA01081 to the University of Bristol, and the Com-
monwealth Scientific and Industrial Research Organisation (CSIRO
Australia) and Bureau of Meteorology (Australia). We are indebted
to E. Dlugokencky for his continuing efforts to produce the NOAA
CH₄ dataset, and for his helpful comments on our manuscript.
NOAA measurements are supported in part by the NOAA Climate
Program Office’s AC4 program and benefited from the technical
assistance of C. Siso, B. Hall, G. Dutton, and J. Elkins.

1. Kirschke S et al. (2013) Three decades of global methane sources and sinks. *Nature Geo- science* 6(10):813–823.
2. Dlugokencky EJ et al. (2003) Atmospheric methane levels off: Temporary pause or a new steady-state? *Geophysical Research Letters* 30(19):3–6.
3. Rigby M et al. (2008) Renewed growth of atmospheric methane. *Geophysical Research Letters* 35(22):L22805.
4. Dlugokencky EJ et al. (2009) Observational constraints on recent increases in the atmo- spheric CH₄ burden. *Geophysical Research Letters* 36:L18803.
5. Hausmann P, Sussmann P, Smale D (2016) Contribution of oil and natural gas production to renewed increase in atmospheric methane (2007–2014): top-down estimate from ethane and methane column observations. *Atmospheric Chemistry and Physics* 16(5):3227–3244.
6. Nisbet EG et al. (2016) Rising atmospheric methane: 2007-2014 growth and isotopic shift. *Global Biogeochemical Cycles* 30(9):1356–1370.
7. Dalsoren SB, Isaksen ISA (2006) CTM study of changes in tropospheric hydroxyl distribution 1990–2001 and its impact on methane. *Geophysical Research Letters* 33:L23811.
8. Voulgarakis A et al. (2013) Analysis of present day and future OH and methane lifetime in the ACCMIP simulations. *Atmospheric Chemistry and Physics* 13(5):2563–2587.
9. Lovelock JE (1977) Methyl chloroform in the troposphere as an indicator of OH radical abun- dance. *Nature* 267(5606):32–32.
10. Prinn RG et al. (2001) Evidence for substantial variations of atmospheric hydroxyl radicals in the past two decades. *Science* 292:1882–1888.
11. Prinn RG et al. (2005) Evidence for variability of atmospheric hydroxyl radicals over the past quarter century. *Geophysical Research Letters* 32:L07809.
12. Bousquet P, Hauglustaine DA, Peylin P, Carouge C, Ciais P (2005) Two decades of OH vari- ability as inferred by an inversion of atmospheric transport and chemistry of methyl chloroform. *Atmospheric Chemistry and Physics* 5:2635–2656.
13. Montzka SA et al. (2011) Small Interannual Variability of Global Atmospheric Hydroxyl. *Sci- ence* 331(6013):67–69.
14. McNorton J et al. (2016) Role of OH variability in the stalling of the global atmospheric CH₄ growth rate from 1999 to 2006. *Atmospheric Chemistry and Physics* 16(12):7943–7956.
15. Krol M, Lelieveld J (2003) Can the variability in tropospheric OH be deduced from mea- surements of 1,1,1-trichloroethane (methyl chloroform)? *Journal of Geophysical Research* 108(D3):4125.
16. Pison I, Bousquet P, Chevallerier F, Szopa S, Hauglustaine D (2009) Multi-species inversion of CH₄, CO and H₂; emissions from surface measurements. *Atmospheric Chemistry and Physics* 9(14):5281–5297.
17. Krol MC et al. (2003) Continuing emissions of methyl chloroform from Europe. *Nature* 421(6919):131–135.
18. Reimann S et al. (2005) Low European methyl chloroform emissions inferred from long-term atmospheric measurements. *Nature* 433(7025):506–8.
19. McCulloch A, Midgley PM (2001) The history of methyl chloroform emissions: 1951-2000. *Atmospheric Environment* 35(31):5311–5319.
20. Liang Q et al. (2014) Constraining the carbon tetrachloride (CCl₄) budget using its global trend and inter-hemispheric gradient. *Geophysical Research Letters* 41(14):5307–5315.
21. Prinn RG et al. (2000) A history of chemically and radiatively important gases in air deduced from ALE/GAGE/AGAGE. *Journal of Geophysical Research* 105(D14):17751–17792.
22. White J, Vaughn BH (2015) University of Colorado, Institute of Arctic and Alpine Research (INSTAAR), Stable Isotopic Composition of Atmospheric Methane (13c) from the NOAA ESRL Carbon Cycle Cooperative Global Air Sampling Network, 1998-2014, Version: 2015-08-03.
23. Miller JB et al. (2002) Development of analytical methods and measurements of 13c/12c in atmospheric CH₄ from the NOAA Climate Monitoring and Diagnostics Laboratory Global Air Sampling Network. *Journal of Geophysical Research* 107(D13).
24. Rigby M et al. (2013) Re-evaluation of the lifetimes of the major CFCs and CH₃cc13 using atmospheric trends. *Atmospheric Chemistry and Physics* 13(5):2691–2702.
25. UNEP (2016) UNEP Ozone Secretariat Data Centre.
26. Schaefer H et al. (2016) A 21st-century shift from fossil-fuel to biogenic methane emissions indicated by 13ch4. *Science* 352(6281):80–84.
27. Turner AJ et al. (2016) A large increase in U.S. methane emissions over the past decade inferred from satellite data and surface observations. *Geophysical Research Letters* 43(5):2218–2224.
28. Bergamaschi P et al. (2013) Atmospheric CH₄ in the first decade of the 21st century: Inverse modeling analysis using SCIAMACHY satellite retrievals and NOAA surface measurements. *Journal of Geophysical Research: Atmospheres* 118(13):7350–7369.

621	29. Tans PP (1997) A note on isotopic ratios and the global atmospheric methane budget. <i>Global Biogeochemical Cycles</i> 11(1):77.	683
622	30. Helmig D et al. (2016) Reversal of global atmospheric ethane and propane trends largely due to US oil and natural gas production. <i>Nature Geoscience</i> 9(7):490–495.	684
623	31. Franco B et al. (2015) Retrieval of ethane from ground-based FTIR solar spectra using improved spectroscopy: Recent burden increase above Jungfraujoch. <i>Journal of Quantitative Spectroscopy and Radiative Transfer</i> 160:36–49.	685
624	32. Patra PK et al. (2014) Observational evidence for interhemispheric hydroxyl-radical parity. <i>Nature</i> 513(7517):219–223.	686
625	33. Wennberg PO, Peacock S, Randerson JT, Bleck R (2004) Recent changes in the air-sea gas exchange of methyl chloroform. <i>Geophysical Research Letters</i> 31(16):3–6.	687
626	34. Brenninkmeijer CAM, Lowe DC, Manning MR, Sparks RJ, van Velthoven PFJ (1995) The 13c, 14c, and 18o isotopic composition of CO, CH4, and CO2 in the higher southern latitudes lower stratosphere. <i>Journal of Geophysical Research</i> 100(D12):26163–26172.	688
627	35. Allan W, Struthers H, Lowe DC (2007) Methane carbon isotope effects caused by atomic chlorine in the marine boundary layer: Global model results compared with Southern Hemisphere measurements. <i>Journal of Geophysical Research</i> 112(D4).	689
628	36. Saueressig G, Crowley JN, Bergamaschi P, Brenninkmeijer CAM, Fischer H (2001) Carbon 13 and D kinetic isotope effects in the reactions of CH4 with O(1d) and OH: New Laboratory measurements and their implications for the isotopic composition of stratospheric methane. <i>Journal of Geophysical Research</i> 106(D19):23127–23138.	690
629	37. Lassey KR, Etheridge DM, Lowe DC, Smith AM, Ferretti DF (2007) Centennial evolution of the atmospheric methane budget: what do the carbon isotopes tell us? <i>Atmospheric Chemistry and Physics</i> 7(8):2119–2139.	691
630	38. Hastings WK (1970) Monte Carlo sampling methods using Markov chains and their applications. <i>Biometrika</i> 57(1):97–109.	692
631	39. Craig H (1957) Isotopic standards for carbon and oxygen and correction factors for mass-spectrometric analysis of carbon dioxide. <i>Geochimica et Cosmochimica Acta</i> 12(1-2):133–149.	693
632	40. Dlugokencky EJ, Steele LP, Lang PM, Masarie Ka (1994) The growth rate and distribution of atmospheric methane. <i>Journal of Geophysical Research</i> 99(D8):17021–17043.	694
633	41. O'Doherty S et al. (2001) In situ chloroform measurements at Advanced Global Atmospheric Gases Experiment atmospheric research stations from 1994 to 1998. <i>Journal of Geophysical Research</i> 106(D17):20429–20444.	695
634	42. Miller BR et al. (2008) Medusa : A Sample Preconcentration and GC / MS Detector System for in Situ Measurements of Atmospheric Trace Halocarbons , Hydrocarbons , and Sulfur Compounds. <i>Analytical Chemistry</i> 80(5):1536–1545.	696
635	43. Cunnold DM et al. (2002) In situ measurements of atmospheric methane at GAGE/AGAGE sites during 1985–2000 and resulting source inferences. <i>Journal of Geophysical Research</i> 107(D14):4225.	697
636	44. Stevens CM, Rust FE (1982) The carbon isotopic composition of atmospheric methane. <i>Journal of Geophysical Research</i> 87(C7):4879.	698
637	45. Tyler SC (1986) Stable carbon isotope ratios in atmospheric methane and some of its sources. <i>Journal of Geophysical Research</i> 91(D12):13232.	699
638	46. Lowe DC, Brenninkmeijer CAM, Tyler SC, Dlugokencky EJ (1991) Determination of the isotopic composition of atmospheric methane and its application in the Antarctic. <i>Journal of Geophysical Research</i> 96(D8):15455.	700
639	47. Patra PK et al. (2011) TransCom model simulations of CH4 and related species: linking transport, surface flux and chemical loss with CH4 variability in the troposphere and lower stratosphere. <i>Atmospheric Chemistry and Physics</i> 11(24):12813–12837.	701
640	48. Cunnold DM et al. (1983) The Atmospheric Lifetime Experiment 3. Lifetime Methodology and Application to Three Years of CFC13 Data. <i>Journal of Geophysical Research</i> 88(C13):8379–8400.	702
641	49. Cunnold DM et al. (1994) Global trends and annual releases of CCl3f and CCl2f2 estimated from ALE/GAGE and other measurements from July 1978 to June 1991. <i>Journal of Geophysical Research</i> 99(D1):1107–1126.	703
642	50. Sander SP et al. (2011) Chemical Kinetics and Photochemical Data for Use in Atmospheric Studies: Evaluation Number 17, (NASA Jet Propulsion Laboratory), Technical Report 17.	704
643	51. Spivakovskiy CM et al. (2000) Three-dimensional climatological distribution of tropospheric OH: Update and evaluation. <i>Journal of Geophysical Research</i> 105(D7):8931–8980.	705
644	52. Morice CP, Kennedy JJ, Rayner NA, Jones PD (2012) Quantifying uncertainties in global and regional temperature change using an ensemble of observational estimates: The HadCRUT4 data set. <i>Journal of Geophysical Research: Atmospheres</i> 117:D08101.	706
645	53. Chipperfield MP et al. (2013) Model Estimates of Lifetimes in SPARC Report on the Lifetimes of Stratospheric Ozone-Depleting Substances, Their Replacements, and Related Species, eds. Reimann S, Ko. MKW, Newman PA, Strahan SE. (WMO/ICSU/IOC World Climate Research Programme, Zurich, Switzerland) No. SPARC Report No. 6, WCRP-15/2013.	707
646	54. Ganesan AL et al. (2014) Characterization of uncertainties in atmospheric trace gas inversions using hierarchical Bayesian methods. <i>Atmospheric Chemistry and Physics</i> 14(8):3855–3864.	708
647	55. Roberts G, Gelman A, Gilks W (1997) Weak convergence and optimal scaling of random walk Metropolis algorithms. <i>The Annals of Applied Probability</i> 7(1):110–120.	709
648	56. Engel A et al. (2013) Inferred Lifetimes from Observed Trace-Gas Distributions in SPARC Report on the Lifetimes of Stratospheric Ozone-Depleting Substances, Their Replacements, and Related Species, eds. Reimann S, Ko. MKW, Newman PA, Strahan SE. (WMO/ICSU/IOC World Climate Research Programme, Zurich, Switzerland) No. SPARC Report No. 6, WCRP-15/2013.	710
649	57. Whitticar M, Schaefer H (2007) Constraining past global tropospheric methane budgets with carbon and hydrogen isotope ratios in ice. <i>Philosophical Transactions of the Royal Society A</i> 365:1793–1828.	711
650	58. Snover AK, Quay PD, Hao WM (2000) The D/H content of methane emitted from biomass burning. <i>Global Biogeochemical Cycles</i> 14(1):11–24.	712
651	59. Rigby M, Manning AJ, Prinn RG (2012) The value of high-frequency, high-precision methane isotopologue measurements for source and sink estimation. <i>Journal of Geophysical Research</i> 117(D12):1–14.	713
652	60. Levin I et al. (2012) No inter-hemispheric $\delta^{13}C_{CH4}$ trend observed. <i>Nature</i> 486(7404):E3–E4.	714
653	61. Lassey KR, Lowe DC, Manning MR (2000) The trend in atmospheric methane 13c and implications for isotopic constraints on the global methane budget. <i>Global Biogeochemical Cycles</i> 14(1):41–49.	715
654		716
655		717
656		718
657		719
658		720
659		721
660		722
661		723
662		724
663		725
664		726
665		727
666		728
667		729
668		730
669		731
670		732
671		733
672		734
673		735
674		736
675		737
676		738
677		739
678		740
679		741
680		742
681		743
682		744